

## Efficient Conversion of Maltose into Sorbitol over Magnetic Catalyst in Extremely Low Acid

Jun Zhang, Jibiao Li, Shubin Wu,\* Ying Liu \*

Ni/Cu/Al/Fe hydrotalcite precursor was synthesized by a co-precipitation method. The activity of the reduced precursor for one-step conversion of maltose into sorbitol in the presence of H<sub>2</sub> and extremely low phosphoric acid was investigated. XRD and XPS tests provided the essential properties of the precursor and prepared magnetic catalyst. Effects of various processing parameters towards the reaction performance were studied in detail. A desired sorbitol yield of 93.1% was attained at 458 K for 3 h with a catalyst dosage of 20%. A catalyst recycling experiment demonstrated that Ni<sub>4.63</sub>Cu<sub>1</sub>Al<sub>1.82</sub>Fe<sub>0.79</sub> was a better catalyst and could be reused three or four times. The specific reasons for catalyst deactivation were considered in depth.

*Keywords:* Hydrotalcite precursor; Maltose; Magnetic catalyst; Sorbitol

*Contact information:* State Key Laboratory of Pulp and Paper Engineering, South China University of Technology, Guangzhou, Guangdong, 510640, China;

\* *Corresponding author:* shubinwu@scut.edu.cn, amyliu@scut.edu.cn

### INTRODUCTION

The depletion of fossil fuel reserves and their impact on the environment have led to an increasing interest in sustainable development. Recent research on the production and conversion of sorbitol has gained wide attention, since it is known as one of the 12 important target chemicals that the U.S. Department of Energy (US-DOE) selected in their biomass program (Werpy *et al.* 2004). Sorbitol, being the most commonly used sugar alcohol, holds the biggest market share among similar polyols, which are widely used in medicine and in the food and chemical industries. For instance, it is an important precursor for the manufacture of L-ascorbic acid, which consumes almost 15% of the world's sorbitol production (Gallezot *et al.* 1994). Most importantly, high value-added chemicals such as light paraffins and H<sub>2</sub> can be obtained through aqueous phase reforming of sorbitol (Huber *et al.* 2004).

In recent research, noble metal catalysts such as Ru/C (Crezee *et al.* 2003; Gallezot *et al.* 1998) and Pt/C (Yan *et al.* 2006) have been found to exhibit high yield and selectivity towards sorbitol. For glucose hydrogenation, the yield and selectivity of sorbitol can reach above 90% under the catalyzing of Ru-based catalysts (Zhang *et al.* 2011). However, the selectivity to sorbitol decreased markedly during the hydrolytic hydrogenation of cellulose, and downstream molecules such as ethylene glycol and propylene glycol were produced at the same time (Palkovits *et al.* 2010). Furthermore, the formation of these lower alcohols was hard to avoid during the hydrogenation process at temperatures of about 473 K. In previous work, Ru/C catalyst combined with extremely low acid was developed for direct conversion of cellobiose into sorbitol, and

an optimized sorbitol yield of 87.1% was attained at 458 K and 3 MPa H<sub>2</sub> (Zhang *et al.* 2012). On the other hand, the preparation costs for these catalysts are too high and will tend to limit industrial applications of sorbitol production. Concerning the high cost of cellobiose, the use of maltose as raw material for the production of sorbitol is more promising in biomass utilization.

Herein, the cheap Ni/Cu/Al/Fe hydrotalcite was synthesized and used as the precursor for the preparation of the hydrogenation catalyst, which can also be easily separated in magnetic fields. The prepared magnetic catalyst was used for efficient hydrolytic hydrogenation of maltose in extremely dilute H<sub>3</sub>PO<sub>4</sub>. The effects of various processing conditions on one-step conversion of maltose into sorbitol are studied in more detail to find the optimal sorbitol yield.

## EXPERIMENTAL

### Materials

5 wt.% Ru/C, 5 wt.% Pd/C, 5 wt.% Pt/C, maltose, and sorbitol were purchased from Shanghai Jingchun Reagent. All chemicals used were of analytical grade.

### Catalysts Preparation

Ni/Cu/Al/Fe hydrotalcite-like compound (HTlc) was synthesized with use of a co-precipitation method (Velu *et al.* 1997). An aqueous solution (150 mL) containing appropriate amounts of Cu(NO<sub>3</sub>)<sub>2</sub>•6H<sub>2</sub>O, Ni(NO<sub>3</sub>)<sub>2</sub>•6H<sub>2</sub>O, Fe(NO<sub>3</sub>)<sub>3</sub>•9H<sub>2</sub>O, and Al(NO<sub>3</sub>)<sub>3</sub>•9H<sub>2</sub>O with cations concentration of 1 mol/L was added dropwise with vigorous stirring into 150 mL of NaOH and Na<sub>2</sub>CO<sub>3</sub> solutions ([OH<sup>-</sup>] = 2 ([Cu<sup>2+</sup>] + [Ni<sup>2+</sup>] + [Al<sup>3+</sup>] + [Fe<sup>3+</sup>]), [CO<sub>3</sub><sup>2-</sup>] = 0.5 ([Al<sup>3+</sup>] + [Fe<sup>3+</sup>])). The addition took about 0.5 h. The pH was kept between 8.5 and 10. The resulting slurry was aged at 333 K for 10 h. The precipitate was filtered, washed thoroughly with distilled water, and then dried at 353 K for 24 h. Before the test, the samples were reduced at 923 K for 3 h in an H<sub>2</sub> flow. The chemical composition of hydrotalcite precursor was identified by ICP-AES analysis, and the obtained catalyst was denoted as Ni<sub>4.63</sub>Cu<sub>1</sub>Al<sub>1.82</sub>Fe<sub>0.79</sub>.

### Catalyst Characterization

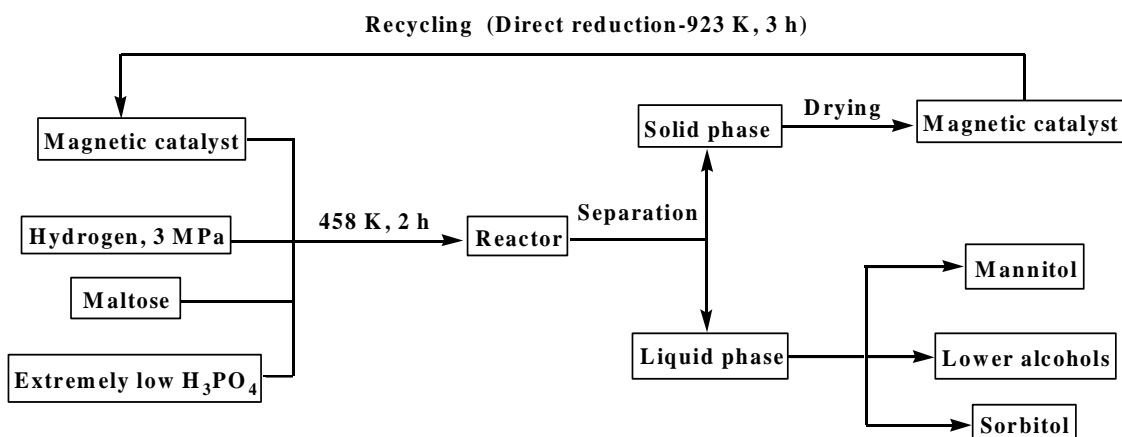
Chemical analysis was carried out on a Thermo Elemental ICP-AES spectrometer after dissolution of the solid sample in an HNO<sub>3</sub> solution. X-ray powder diffraction (XRD) was performed in a Bruker D8 Advance X-Ray Diffractometer using Cu K $\alpha$  radiation. The operating voltage and current were 40 kV and 40 mA, respectively. The step length was 0.02° with a scanning rate of 2°/min. The crystallite size was calculated by XRD-line broadening using the Scherrer equation (Klug and Alexander 1974). X-ray photoelectron spectroscopy (XPS) measurements were made with a Kratos Ultra system employing an Al K $\alpha$  radiation source. The binding energies for each spectrum were calibrated with a C1s spectrum of 284.6 eV. Survey spectra for each sample over a binding energy range of 0 to 1100 eV were recorded at a pass energy of 160 eV and a

resolution of 1 eV per step. High-resolution spectra of Cu 2p and Ni 2p were recorded at a pass energy of 40 eV and a resolution of 0.1 eV per step, for quantitative measurements of binding energy. The pore size and volume of used catalysts were determined following the standard nitrogen adsorption method using a Micromeritics Tristar 3020 instrument. Specific surface areas were calculated using the BET equation. Prior to analyses, all samples were degassed at 393 K and  $10^{-4}$  Torr pressure for 8 h to evacuate the physically adsorbed moisture. The carbon contents of recycled samples were determined by using XRF (X-ray Fluorescence Spectrometer) technique.

The measurement of acidity of the catalyst was carried out in a Micromeritics AutochemII 2920 chemisorption analyzer following an  $\text{NH}_3$  temperature-programmed desorption (TPD) method. The sample was heated up to 873 K at the rate of 15 K/min and kept for 30 min in a flow of He gas (20 mL/min) to remove adsorbed species on the surface. Then the sample was cooled down to 373 K in He flow, followed by adsorption of  $\text{NH}_3$  in 10%  $\text{NH}_3$  gas flow (balance He, 20 mL/min) for 1 h. After flushing with He for 1 h to remove physically adsorbed  $\text{NH}_3$ , the TPD data were measured from 373 K to 873 K with a ramp of 15 K/min.

### Catalytic Reaction

The conversion of maltose to sorbitol was performed with a high pressure reactor (PARR 5500). For each run, maltose, catalysts, and 0.08 wt.%  $\text{H}_3\text{PO}_4$  were put into the reactor; then, the reaction was carried out at several temperatures under 3 MPa  $\text{H}_2$  for a certain time with a stirring rate of 600 rpm. After reaction, the reactor was cooled down rapidly with ice water to room temperature; then, the liquid product was collected by filtration and put in a refrigerator set to 278 K. The used catalyst was reduced again before the next use. A brief schematic process is shown in Scheme 1. The liquid products were analyzed by IC (Dionex ICS-3000) with a CarboPac PA20 Column. The eluents were NaOH and  $\text{H}_2\text{O}$  with a flow rate of 0.25 mL/min. The sample loop had a volume of 50  $\mu\text{L}$ . The column temperature was 303 K.



**Scheme 1.** Schematic process for the conversion of maltose to sorbitol

## RESULTS AND DISCUSSION

### Catalyst Characterization

#### XRD test

Phase identification of the prepared samples was performed by XRD, and the results are given in Fig. 1. The XRD pattern of the catalyst precursor (the inset in Fig. 1) exhibited sharp and symmetrical reflections for (003), (006), and (113) planes and broad and asymmetric reflections for (012), (015), and (018) planes, characteristic of a well-crystallized HT in carbonate form (Courty *et al.* 1982; Sate *et al.* 1988). The peaks at 11.7, 23.3, 35.0, 39.0, 47.2, and 61.6 could be assigned to the (003), (006), (012), (015), (018), and (113) diffractions of HTlc, respectively. No isolated phases of individual Ni, Cu, Al, and Fe hydroxides were observed in the XRD patterns of  $\text{Ni}_{4.63}\text{Cu}_1\text{Al}_{1.82}\text{Fe}_{0.79}\text{-HTlc}$ , suggesting that Ni and Cu had been homogeneously incorporated into the matrixes of  $\text{Ni}_{4.63}\text{Cu}_1\text{Al}_{1.82}\text{Fe}_{0.79}\text{-HTlc}$ .

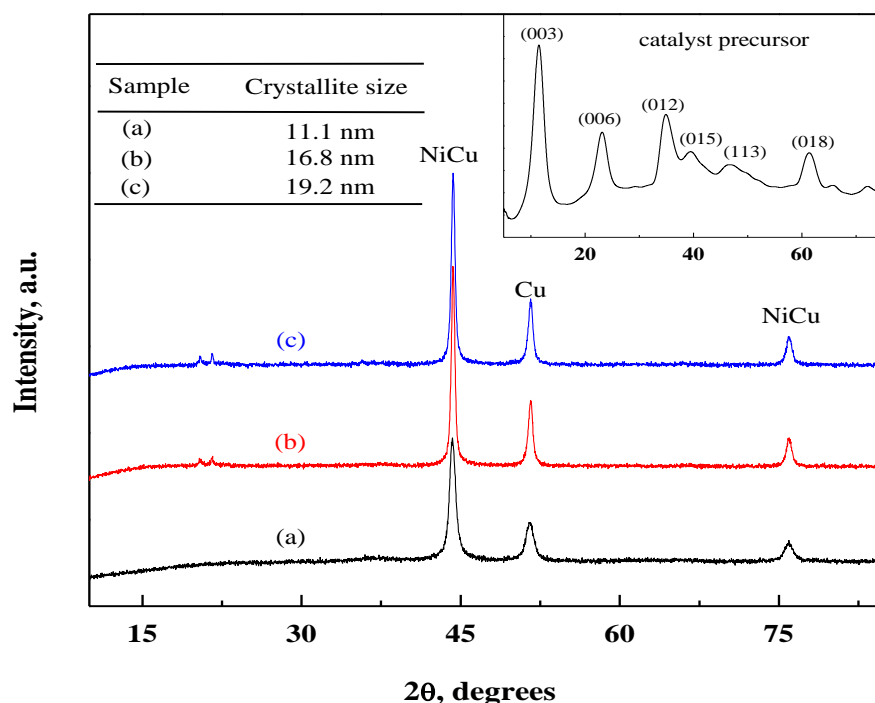


**Fig. 1.** Powder XRD patterns of used catalysts: (a) fresh; (b) used once; (c) used twice. (Inset): powder XRD pattern of catalyst precursor

For the reduced sample, peaks corresponding to planes (200) at  $2\theta$  of  $51.7^\circ$  could be clearly observed. These peaks coincided with those in files JCPDS 4-836, indicating the presence of metallic Cu in the face-centered-cubic structure. Besides, peaks corresponding to planes (111) at  $2\theta$  of  $44.2^\circ$  and planes (220) at  $2\theta$  of  $75.8^\circ$  indicated the formation of Cu-Ni solid solution, which could be assigned to a Ni-rich alloy. These results are in line with those reported by Rao *et al.* (2004), Wu (2007), and Wu *et al.* (2007) in relation to the peak positions in the XRD diagram of the Cu-Ni alloy. Two reflections at around  $20^\circ$  could be assigned to the diffraction peaks of carbon, indicating that much carbon was adsorbed on the catalyst during recycling experiments. It can be

seen that the corresponding crystallite sizes of the reduced catalysts obviously increased with increasing recycling time, as given in the table in Fig. 1. That may be caused by the effect of sintering under high temperature, which would lead to the growth of crystal particle size.

#### XPS analysis

The main reason for conducting XPS analysis was to obtain information regarding the chemical environment presented in the prepared catalyst. High-resolution scans of the XPS spectra of Cu 2p and Ni 2p with different intensity scales as ordinate are shown in Fig. 2. Four obvious peaks in the diagram of Cu 2p were found in the reduced sample, representing various valence states of the Cu element. Two shake-up lines appeared at 940.6 and 960.7 eV separately. The binding energies (BE) of Cu 2p<sub>3/2</sub> and 2p<sub>1/2</sub> were around 932.3 and 953.2 eV, respectively, which were very close to that of Cu<sup>0</sup>. Note that the binding energies of metallic Cu are around 932.6 and 953.8 eV (Moretti *et al.* 1989; Strohmeier *et al.* 1985). For the Ni element, the obtained binding energies were around 852.8 and 869.9 eV, demonstrating the presence of Ni 2p<sub>3/2</sub> and 2p<sub>1/2</sub>, respectively. The binding energy of Ni 2p<sub>3/2</sub> in pure NiO is 854.5 eV, while for the NiAl<sub>2</sub>O<sub>4</sub> spinel it appears at 856 eV (Lenglet *et al.* 1997). As for the reduced catalyst, two peaks were observed at binding energies of about 853.5 and 871.0 eV that were among those of Ni<sup>0</sup> and Ni<sup>2+</sup>. Two satellites at binding energies of about 860.0 and 878.0 eV were observed. It can be seen that the BE of 2p electrons of Cu<sup>0</sup> were lower than 932.6 and 953.8 eV. Meanwhile, those of Ni<sup>0</sup> were 853.5 and 871.0 eV higher than 852.8 and 869.9 eV. It was inferred that the stronger electronic negativity of metallic Cu led to electrons transferring from Ni to Cu, so electron-rich of metallic Cu led to a red shift of 2p electrons. The above results further demonstrated the existence of NiCu alloy, because the interaction between Cu and Ni in alloy might lead to an influence on the electronic density in outer layers of metallic Cu and Ni.

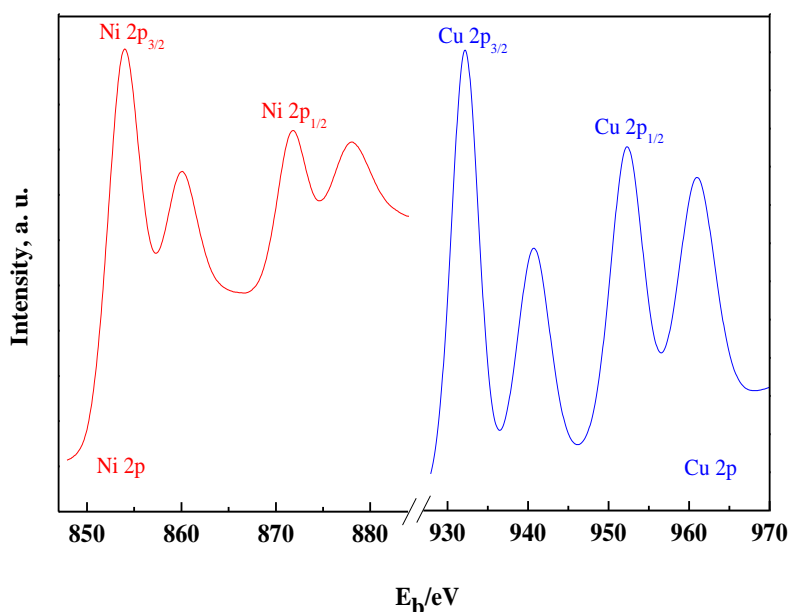
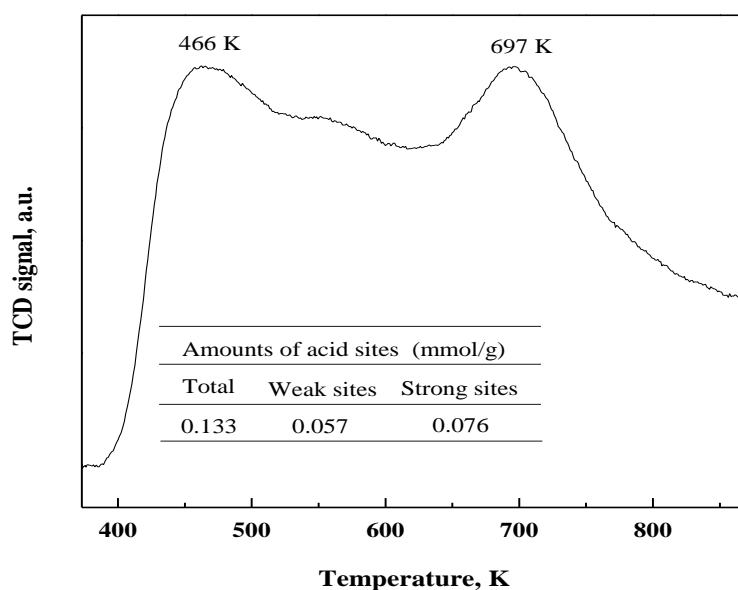


Fig. 2. XPS spectra of Cu 2p and Ni 2p of catalyst

*NH<sub>3</sub>-TPD measurement*

The NH<sub>3</sub>-TPD profile of the prepared catalyst is shown in Fig. 3. NH<sub>3</sub> molecules can be adsorbed on the acid sites of catalysts and be removed during the heating process. Acid sites of magnetic catalyst were distributed in two desorption regions at about 400 K to 600 K and 650 K to 750 K. The source of acidity was attributed to the presence of Al and Fe in hydrogenation catalyst. Temperatures of NH<sub>3</sub> desorption peaks and the quantities of total acid sites are summarized in Fig. 3. The total amount of acid sites was 0.133 mmol/g, and both the amounts of weak and strong sites were relatively low. It was speculated that the hydration reaction was primarily completed under the catalyzing of extremely low acid. The acid sites of catalyst might have promoting effect on hydrogenation reaction, because weakly basic C=O of glucose could be activated by Brønsted acid.



**Fig. 3.** NH<sub>3</sub>-TPD profile of magnetic catalyst

*Properties of recycled catalysts*

The essential characteristics of recycled catalysts were studied in detail to investigate the specific reasons for catalyst deactivation (seen Table 1).

**Table 1.** Properties of Recycled Catalysts

Catalyst	Fresh	Used once	Used twice
BET surface area, m <sup>2</sup> /g	56.45	40.78	32.64
Pore volume, cm <sup>3</sup> /g	0.19	0.13	0.096
Pore size, nm	13.26	13.12	13.15
<sup>a</sup> Cu, mg/L	< 0.1	< 0.1	< 0.1
<sup>a</sup> Ni, mg/L	4.83	11.49	18.57
Carbon content, %	27.18	33.03	35.52

<sup>a</sup> ICP-AES analysis of residual Cu and Ni contents in corresponding reaction solution.

The BET surface area and pore volume decreased significantly with the recycling of magnetic catalyst, which might be attributed to the increased amount of adsorbed carbon in used samples. It was found that 4.83 mg/L Ni and little Cu (< 0.1 mg/L) were present in reaction solution after the first use of magnetic catalyst. However, much more Ni was leached into the solution in the successive runs, which would further lower the catalyst activity. It is worth noting that the Cu could be stably present in magnetic catalyst.

### Catalytic Performance for the Conversion of Maltose

The influence of reaction temperature on the yield of sorbitol was investigated with reaction time to find the optimum conditions to increase the sorbitol yield. It can be observed from Fig. 4 that the reaction temperature played an important role in the reaction process. At the temperature of 458 K, the yield of sorbitol grew significantly with the prolonging of reaction time. The highest level of 93.3% in sorbitol yield was achieved at 458 K after a reaction of 2 h. However, the sorbitol yield obviously decreased with increasing temperature from 458 to 478 K after the same reaction time, especially for the temperature of 478 K. It must be pointed out that sorbitol will be decomposed to some extent at higher temperatures in the H<sub>2</sub> atmosphere, and much lower alcohols are formed during the reaction. Therefore, excess elevation of temperature is unfavorable for selection of the desired reaction.

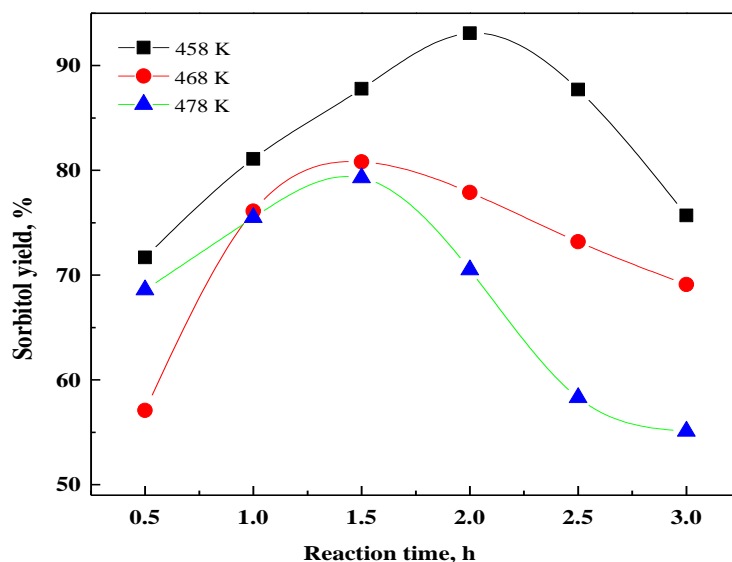


**Fig. 4.** Effect of reaction temperature on the yield of sorbitol with reaction time; 0.25 g maltose, 0.05 g catalyst, 25 mL 0.08 wt.% H<sub>3</sub>PO<sub>4</sub>, 3 MPa H<sub>2</sub>

Catalyst loading is an important parameter that needs to be optimized to increase the sorbitol yield. The experiments were conducted at three different catalyst loadings (20, 30, and 40%) as a function of reaction time, and the results are given in Fig. 5. One can observe that the sorbitol yield was higher for higher catalyst loading during the first 1.5 h of the reaction. This effect was substantial, and the sorbitol yield increased from 80.8 to 88.5% after the reaction time of 1.5 h when increasing the catalyst loading from 20 to 30%. A possible explanation for this is that the increased total number of active

sites led to a faster reaction rate to promote the conversion of maltose into sorbitol. With the further increase of the amount of magnetic catalyst to 40%, the sorbitol yield decreased significantly in the initial stage at the reaction temperature of 468 K. It was inferred that much produced sorbitol was further converted into lower alcohols (over 15% in total) under such high temperature in the hydrogen atmosphere. However, it can be observed that further increasing the reaction time was unfavorable for the direct conversion of maltose into sorbitol due to the reaction of deep hydrogenolysis.

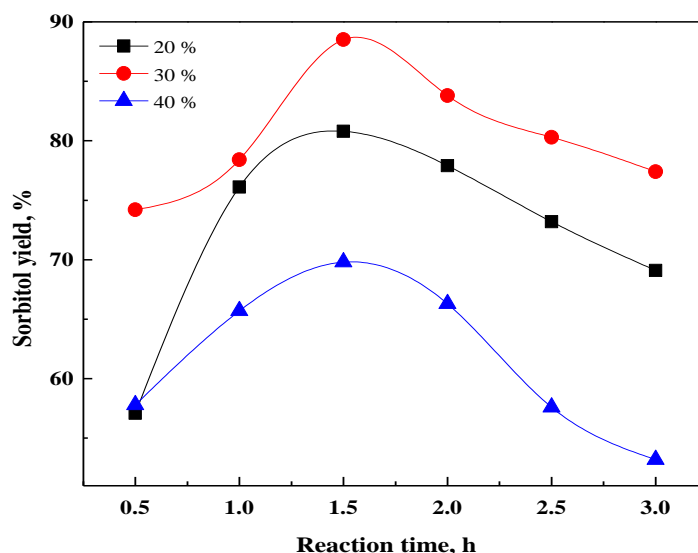


**Fig. 5.** Effect of catalyst dosage on the yield of sorbitol with reaction time; 0.25 g maltose, catalyst ( 20%–0.05 g , 30%–0.075 g, 40%–0.1 g), 25 mL 0.08 wt.%  $\text{H}_3\text{PO}_4$ , 468 K, 3 MPa  $\text{H}_2$

The long-term stability of the heterogeneous catalyst is an extremely important characteristic for practical usage to reduce production costs. After the reaction was finished, the spent magnetic catalyst was separated from the liquid products and was reduced in  $\text{H}_2$  atmosphere again before the next use. As seen from Fig. 6, the yield of sorbitol decreased from 93.1% to around 84.0% in the following two runs, indicating that the catalytic activity of the catalyst had not been completely recovered after direct reduction. However, an obvious decrease in sorbitol yield from 83.5% to 75.5% was observed in the fourth run, which reached about 81.1% of that obtained for the fresh catalyst. This may be due to partial loss of active Ni sites in the catalyst during catalysis. In addition, it is proposed that the recycled samples had larger crystallite size due to the effect of sintering (as seen in Fig. 1). The BET surface area and pore volume of used samples also decreased significantly in recycling experiments, which might be attributed to the increased amount of adsorbed carbon in catalysts. Therefore the reactant might not have made good contact with the catalyst, resulting in an obvious decrease in catalyst activity. The results led to the conclusion that the catalytic activity of the used catalyst could be partly improved in multiple cycles by means of repeated reduction treatment. Accordingly, how to improve the long-term stability of the reduced Cu/Ni/Al/Fe hydrotalcite-like catalyst remains a topic for future exploration.

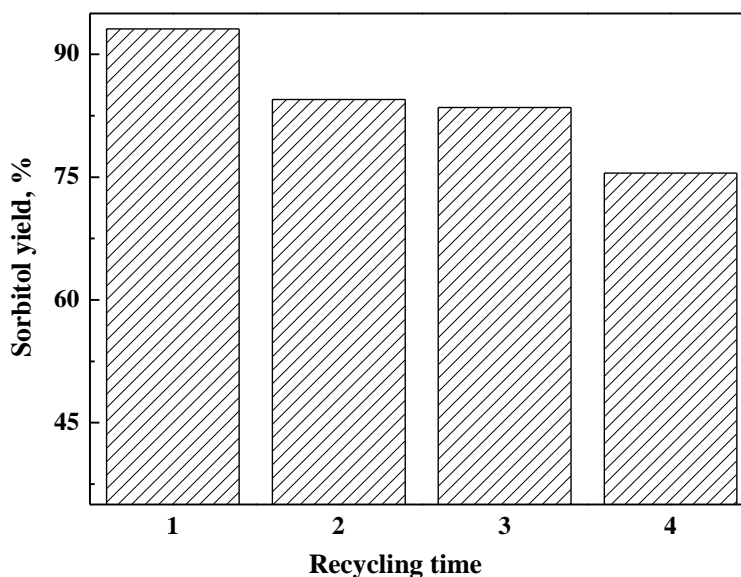


**Fig. 6.** Sorbitol yield as a function of the recycling times of the catalyst; 0.25 g maltose, 0.05 g catalyst, 25 mL 0.08 wt.% H<sub>3</sub>PO<sub>4</sub>, 458 K, 3 MPa H<sub>2</sub>, 2 h

As a comparison, various noble metal catalysts were introduced in one-step conversion of maltose into sorbitol, such as Ru/C, Pt/C, and Pd/C. The obtained results are clearly described in Table 2. Among the tested noble metal catalysts, Ru/C exhibited excellent activity towards sorbitol production, and a sorbitol yield of 94.5% was achieved at a temperature of 458 K. For Pt/C and Pd/C catalysts, the corresponding hydrogenation activities were much lower compared to Ru/C, and much glucose was observed in the final products. However, a yield of 93.1% in sorbitol was attained under the catalyzing of prepared magnetic catalyst as well. Furthermore, the conversion rate of maltose was almost 100% when using Ni<sub>4.63</sub>Cu<sub>1</sub>Al<sub>1.82</sub>Fe<sub>0.79</sub> and Ru/C. Thus the cheap magnetic catalyst also had promising application in sorbitol production as compared with the supported noble metal catalysts that were considered.

**Table 2.** Conversion of Maltose over Various Hydrogenation Catalysts

Catalyst	Ru/C	Pd/C	Pt/C	Ni <sub>4.63</sub> Cu <sub>1</sub> Al <sub>1.82</sub> Fe <sub>0.79</sub>
Sorbitol yield, %	94.5	34.2	41.5	93.1
Glucose yield, %	0	4.5	7.6	0.7

Conditions: 0.25 g maltose, 0.05 g catalyst, 458 K, 25 mL 0.08 wt.% H<sub>3</sub>PO<sub>4</sub>, 3 MPa H<sub>2</sub>, 2 h.

## CONCLUSIONS

1. The present study describes a feasible and environmentally friendly catalytic process for direct conversion of maltose into sorbitol in the presence of magnetic catalyst and extremely low phosphoric acid under an H<sub>2</sub> atmosphere.
2. A sorbitol yield of 93.1% was attained at 458 K for 2 h under 3 MPa H<sub>2</sub>.

3. XRD and XPS characterization of reduced catalysts indicated that the  $\text{Cu}^{2+}$  was completely reduced to  $\text{Cu}^0$ , and little unreduced NiO was found in the reduced samples.
4. A catalyst recycling experiment demonstrated that  $\text{Ni}_{4.63}\text{Cu}_1\text{Al}_{1.82}\text{Fe}_{0.79}$  sustained better catalytic activity, in comparison to Pd/C and Pt/C catalysts, after being reused several times.
5. The BET surface area and pore volume of used samples decreased significantly, and some of the Ni constituting the active Ni sites could be easily leached into the solutions in recycling experiments.

## ACKNOWLEDGMENTS

This work was supported by the supported by National Key Basic Research Program of China (No. 2013CB228101), National Natural Science Foundation of China (No. 31270635), and the National High Technology Research and Development Program of China (863 Program, 2012AA101806).

## REFERENCES CITED

- Courty, P., Durand, D., Freund, E., and Sugier, A. (1982). "C<sub>1</sub>-C<sub>6</sub> alcohols from synthesis gas on copper-cobalt catalysts," *J. Mol. Catal.* 17(2-3), 241-254.
- Crezee, E., Hoffer, B. W., Berger, R. J., Makkee, M., Kapteijn, F., and Moulijn, J. A. (2003). "Three-phase hydrogenation of D-glucose over a carbon supported ruthenium catalyst-mass transfer and kinetics," *Appl. Catal. A: Gen.* 251(1), 1-17.
- Gallezot, P., Cerino, P. J., Blanc, B., Flèche, G., and Fuertes, P. (1994). "Glucose hydrogenation on promoted raney-nickel catalysts," *J. Catal.* 146(1), 93-102.
- Gallezot, P., Nicolaus, N., Flèche, G., Fuertes, P., and Perrard, A. (1998). "Glucose hydrogenation on ruthenium catalysts in a trickle-bed reactor," *J. Catal.* 180(1), 51-55.
- Huber, G. W., Cortright, R. D., and Dumesic, J. A. (2004). "Renewable alkanes by aqueous-phase reforming of biomass-derived oxygenates," *Angew. Chem. Int. Ed.* 43(12), 1549-1551.
- Klug, H. P., and Alexander, L. E. (1974). *X-ray Diffraction Procedures for Polycrystalline and Amorphous Materials*, 2<sup>nd</sup> Ed., Wiley, New York.
- Lenglet, M., Hochu, F., Durr, J., and Tuilier, M. H. (1997). "Investigation of the chemical bonding in 3d<sup>8</sup> nickel (II) charge transfer insulators (NiO, oxidic spinels) from ligand-field spectroscopy, Ni 2p XPS and X-ray absorption spectroscopy," *Solid State Commun.* 104(12), 793-798.
- Moretti, G., Fierro, G., Jacono, M. L., and Porta, P. (1989). "Characterization of CuO-ZnO catalysts by X-ray photoelectron spectroscopy: Precursors, calcined and reduced samples," *Surf. Interface Anal.* 14(6-7), 325-336.

- Palkovits, R., Tajvidi, K., Procelewska, J., Rinaldi, R., and Ruppert, A. (2010). "Hydrogenolysis of cellulose combining mineral acids and hydrogenation catalysts," *Green Chem.* 12(6), 972-978.
- Rao, G. R., Mishra, B. G., and Sahu, H. R. (2004). "Synthesis of CuO, Cu and CuNi alloy particles by solution combustion using carbohydrazide and N-tertiarybutoxy-carbonylpiperazine fuels," *Mater. Lett.* 58(27-28), 3523-3527.
- Sate, T., Fujita, H., Endo, T., and Shimada, M. (1988). "Synthesis of hydrotalcite-like compounds and their physico-chemical properties," *React. Solid.* 5(2-3), 219-228.
- Strohmeier, B. R., Leyden, B. E., Field, R. S., and Hercules, D. M. (1985). "Surface spectroscopic characterization of Cu/Al<sub>2</sub>O<sub>3</sub> catalysts," *J. Catal.* 94(2), 514-530.
- Velu, S., Ramaswamy, V., and Sivasanker, S. (1997). "New hydrotalcite-like anionic clays containing Zr<sup>4+</sup> in the layers," *Chem. Commun.* (21), 2107-2108.
- Werpy, T., Petersen, G., Aden, A., Bozell, J., Holladay, J., Manheim, A., Eliot, D., Lasure, L., and Jones, S. (2004). *Top Value Added Chemicals from Biomass, Vol. 1*, U.S. Department of Energy, Oak Ridge, TN.
- Wu, S. P. (2007). "Preparation of ultra fine nickel-copper bimetallic powder for BME-MLCC," *Microelectron. J.* 38(1), 41-47.
- Wu, S. P., Ni, J., Jiao, L., and Zeng, Z. N. (2007). "Preparation of ultra-fine copper-nickel bimetallic powders with hydrothermal-reduction method," *Mater. Chem. Phys.* 105(1), 71-75.
- Yan, N., Zhao, C., Luo, C., Dyson, P. J., Haichao Liu, H. C., and Kou, Y. (2006). "One-step conversion of cellobiose to C<sub>6</sub>-alcohols using a ruthenium nanocluster catalyst," *J. Am. Chem. Soc.* 128(27), 8714-8715.
- Zhang, J., Lin, L., Zhang, J. H., and Shi, J. B. (2011). "Efficient conversion of D-glucose into D-sorbitol over MCM-41 supported Ru catalyst prepared by a formaldehyde reduction process," *Carbohydr. Res.* 346(11), 1327-1332.
- Zhang, J., Wu, S. B., Li, B., and Zhang, H. D. (2012). "Direct conversion of cellobiose into sorbitol and catalyst deactivation mechanism," *Catal. Commun.* 29, 180-184.

Article submitted: April 3, 2013; Peer review completed: July 9, 2013; Revised version received and accepted: July 25, 2013; Published: July 29, 2013.